PERGAMON

Chemical Engineering Science 56 (2001) 5011–5023

Chemical
Engineering Science

www.elsevier.com/locate/ces

Catalytic effectiveness of irregular interfaces and rough pores: the "land surveyor approximation"

B. Sapoval[a,b,*], J.S. Andrade Jr.[b,c], M. Filoche[a]

[a]Laboratoire de Physique de la Matière Condensée, Ecole Polytechnique, 91128 Palaiseau, France
[b]Centre de Mathématiques et de leurs Applications, Ecole Normale Supérieure de Cachan, 94235 Cachan, France
[c]Departamento de Física, Universidade Federal do Ceará, 60451-970 Fortaleza, Ceará, Brazil

Received 6 September 2000; received in revised form 12 February 2001; accepted 30 April 2001

Abstract

We apply the concept of active zone in Laplacian transport to investigate the steady state mass transfer of a diffusive species towards an arbitrarily irregular catalytic interface. By means of a recently proposed coarse-graining technique, it is possible to compute the reactive flux on the catalytic interface from its geometry alone, without solving the general Laplace problem. As a result, we demonstrate by direct numerical simulation of molecular diffusion and first-order reaction that this method allows one to predict the catalytic effectiveness of a slit-shaped pore with an arbitrary rough geometry and over a wide range of diffusion–reaction conditions. It is found that, contrary to the traditional pseudo-homogeneous approach, the effect of the irregular morphology at the mesoscopic pore level is to modify the reaction rate and not the effective diffusion coefficient. We show that, for all practical situations where the reactant penetration in the pore is significant, a simplified picture of a smooth pore with an effective reactivity K_{eff} can be used to describe the efficiency of a rough pore. Remarkably, K_{eff} is the product of the intrinsic reactivity by a screening factor S, which has an elementary geometrical meaning, namely, the ratio between the real and the apparent surface area. © 2001 Elsevier Science Ltd. All rights reserved.

Keywords: Porous media; Reaction engineering; Diffusion; Microstructure; Modelling; Fractals

1. Introduction

The study of transport phenomena in porous media is a long-standing research subject with many industrial and technological applications. The development of modeling techniques for the description of diffusion and reaction in heterogeneous catalysis represents a real challenge, mainly due to the limitations of the classical pseudo-homogeneous representations (Bird, Stewart, & Lightfoot, 1960; Aris, 1975). These macroscopic models for diffusion–reaction processes can only implicitly account for the geometrical features of real pore spaces Adler, 1992; Sahimi, 1995). For instance, the standard modeling approach is to consider the catalyst particle as a homogeneous system where reactants and products can diffuse (molecular or Knudsen diffusion) and react according to a given effective transport coefficient and an intrinsic reaction mechanism.

It is now clear that the classical diffusion formalism, which is valid for Euclidean geometries, cannot be used as a macroscopic representation of transport phenomena in some disordered media. In the case of certain porous materials, the breakdown of this traditional transport theory can be explained in terms of an intrinsic structural heterogeneity of the complex void space geometry causing significant changes in the diffusional behavior of the system. This departure from the classical behavior is commonly known as *anomalous diffusion* and usually occurs in the form of a sub-diffusive regime (Havlin & Ben-Avraham, 1987; Stauffer & Aharony, 1992). In a recent study (Andrade, Street, Shibusa, Havlin, & Stanley, 1997), the problem of diffusion and reaction in critical percolation networks (Stauffer & Aharony, 1992) has been investigated. The results from extensive simulations clearly indicate that, in the scaling range of the diffusion–reaction process, the effectiveness of real pore catalysts

---

[*] Corresponding author. Laboratoire de Physique de la Matière Condensée, Ecole Polytechnique, 91128 Palaiseau, France.
E-mail address: bernard.sapoval@polytechnique.fr (B. Sapoval).

PII: S0009-2509(01)00165-8

can be largely overestimated if the self-similar aspect of the void space is not taken into consideration.

Under a more general framework, the problem of diffusion and reaction in irregular geometries (e.g., pore trees, pore networks, surface of fractal aggregates and fractal pore spaces) and its consequences on the reactive properties of porous catalysts has been largely investigated (Villermaux, Schweich, & Authelin, 1987; Gutfraind, Sheintuch, & Avnir, 1991; Elias-Kohav, Sheintuch, & Avnir, 1991; McGreavy, Andrade Jr., & Rajagopal, 1992; Gutfraind & Sheintuch, 1992; Giona, 1992; Keil, 1996; Mougin, Pons, & Villermaux, 1996; Gavrilov & Sheintuch, 1997). At the mesoscopic level, in particular, the role played by the pore shape or the local surface morphology on the overall diffusivity and reactivity of the catalyst has already been a subject of interest (Meakin, 1986; Villermaux et al., 1987; Gutfraind et al., 1991; Seri-Levy & Avnir, 1991; Coppens & Froment, 1994, 1997; Coppens, 1999). For instance, fractal models have been used as a more realistic description for the complex roughness geometry of surfaces in the study of Knudsen diffusivity and reactivity of irregular pores (Coppens & Froment, 1995a,b; Santra & Sapoval, 1999). The fractal concept has also been applied to model the surface geometry of some disordered materials, including catalyst supports and adsorbents (Avnir, 1989).

However, a crucial point remains to be better understood: the effect of the nonuniform accessibility of active sites on irregular catalyst surfaces. Due to *screening* effects, even if we assume that the active sites are uniformly distributed in space along the entire surface, the regions corresponding to fins or extended protrusions will display a higher activity as opposed to the deep parts of fjords which are more difficult to access. As a result, under certain diffusion–reaction constraints, the efficiency of the catalyst surface can be substantially different than the one expected from the intrinsic chemical reactivity (i.e., the activity of the nominal surface).

An entirely analogous problem can be found in the context of electrochemistry, but with the benefit that direct experimental evidence is available. The nonuniform activity during the linear transport through irregular interfaces of electrodes can also be explained in terms of a screening effect which is entirely similar to the one observed in heterogeneous catalysis. The extensive research developed on this subject in recent years (Sapoval, 1994; Pfeifer & Sapoval, 1995; Sapoval, 1996) has been mainly devoted to the introduction, calculation and application of the concept of *active zone* in the Laplacian transport to and across irregular interfaces. For example, a new coarse-graining method proposed in Sapoval (1994) allows one to compute the flux through electrode surfaces from their geometry alone, without solving the general Laplace problem. In the present work, we extend the notion of active zone to reactive interfaces of arbitrary shape and demonstrate, by direct numerical simulation, that this coarse-graining technique provides consistent predictions for the activity of catalyst surfaces. Furthermore, for the case of an arbitrary irregular interface playing the role of roughness in a reactive pore, we show analytically that the catalyst effectiveness is strongly influenced by the surface geometry, whatever the range of diffusion–reaction conditions. When compared with the traditional approach of a smooth pore model, our results indicate that one can erroneously estimate the effectiveness of catalyst materials if the geometrical inhomogeneities of the active surface are not considered properly.

This paper is organized as follows. In Section 2, we discuss the problem of the activity of an irregular catalyst surface which represents a typical wall element of a rough pore. We introduce the "land surveyor approximation" (LSA), and compare the predictions of this technique with the numerical solution obtained for the reactive activity of a particular case, the random Koch curve.

In Section 3, we apply the land surveyor approximation to calculate the effectiveness of an idealized one-dimensional rough pore and compare this with the classical smooth pore approximation. In particular, it is found that the pore roughness contributes to the "falsification" of the activation energy (Froment & Bischoff, 1990; Thomas & Thomas, 1997). This analysis is then extended to the problem of catalyst effectiveness of a deep rough pore in two dimensions. Finally, in Section 4, some conclusions and perspectives for future work are presented.

2. The effectiveness of an irregular catalyst wall

We consider the two-dimensional steady state problem of reactant species A diffusing through a neutral solvent from a source line of length L towards an irregular catalytic interface of perimeter L_p (see Fig. 1a). At this interface, A molecules are converted to $A^\star$ by means of a chemical reaction with first-order kinetics. Measurable quantities can be adequately defined if we introduce the thickness b of the reacting cell along the third dimension. In the bulk of the reacting cell, the diffusion of species A obeys Fick's law, $\vec{J}(\vec{r}) \equiv -D\vec{\nabla}C$, where $\vec{J}$ represents the mass flux vector field, $C(\vec{r})$ is the local concentration at position $\vec{r}$ and D is the molecular diffusion coefficient. Under steady state conditions, the concentration field of the reactant species satisfies the stationary diffusion equation $\nabla^2 C = 0$. For the boundary conditions, we assume a constant concentration of A equal to C_S at the source line, whereas at the active interface, the depletion rate of A follows $J_n \equiv -K_s C$, where K_s is the *intrinsic* surface reaction rate coefficient. In this system, the mass transport of species A is limited by two processes: (i) molecular diffusion from the source through the bulk of the cell, and (ii) the finite reaction rate at the catalytic interface. Due

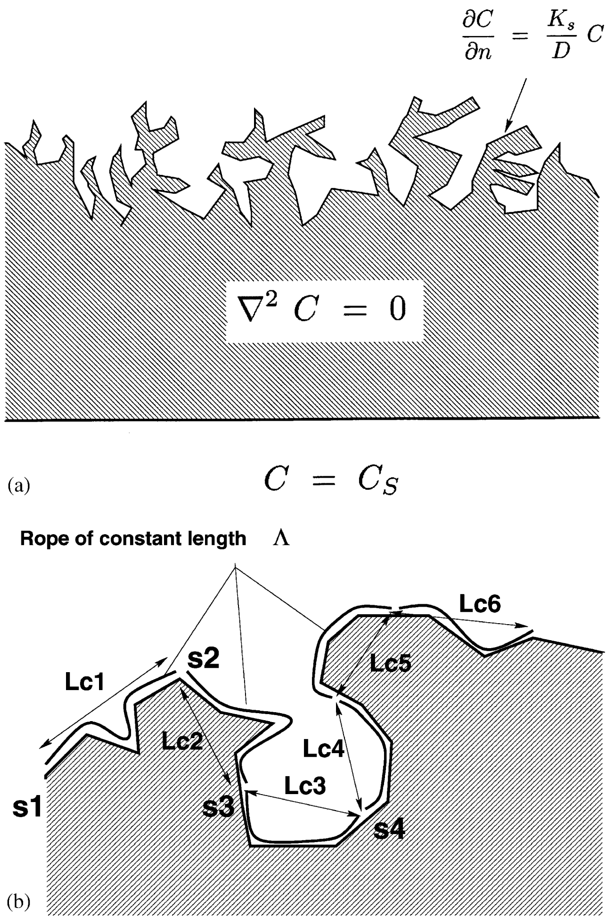

Fig. 1. (a) Schematic representation of the catalytic pore wall under study. The reactive interface presents an irregular geometry. The concentration field of reactant obeys the Laplace equation in the bulk. A constant concentration C_S is maintained at the source line. The boundary condition at the interface is $\partial C/\partial n = K_s C/D$. (b) Schematic representation of the coarse-graining or finite renormalization procedure used in the "land surveyor approximation" (LSA). Successive ropes of length Λ determine successive chords of lengths $L_{c1}, L_{c2}, \ldots$.

to mass conservation, the reaction rate must be equal to the diffusive flux reaching the active interface from the bulk, $D\,\partial C/\partial n = K_s C$. As a consequence, the boundary condition at this point can be written as

$$\frac{\partial C}{\partial n} = \frac{K_s}{D} C. \tag{1}$$

This introduces a finite length scale $\Lambda \equiv D/K_s$ in the problem. In analogy with previous studies on electrodes (Sapoval, 1996), we can also define here an overall conductance for the diffusion–reaction cell as $G_{\text{cell}} = \Phi_{\text{tot}}/C_S$, where Φ_{tot} is the total mass flow of species A penetrating in the system. Due to the linearity of the problem, it is always possible to express the cell resistance, $1/G_{\text{cell}}$, in terms of two other resistances in series,

$$\frac{1}{G_{\text{cell}}} = \frac{1}{G_B} + \frac{1}{G_I}. \tag{2}$$

Here, G_B is the bulk conductance which can be calculated as the overall conductance if the cell is subjected to the boundary condition $C = 0$ at the catalyst interface (i.e., assuming that $K_s \to \infty$). G_B should then be directly proportional to the molecular diffusivity D and depend upon the geometry of the cell. G_I, in turn, is the conductance of the reactive interface and depends on D, on the interface geometry as well as on the reaction rate coefficient K_s. Previous simulations indicate that G_I is weakly dependent on the average distance d between the interface and the source line (Sapoval, Filoche, Karamanos, & Brizzi, 1999). Moreover, we consider here the situation in which d is sufficiently small, so that the term $1/G_B$ can be neglected in Eq. (2). Therefore, for all practical purposes, the activity of the interface can be evaluated only in terms of the conductance G_I.

In conditions of weak diffusional restrictions to mass transfer (large Λ values), the screening effect of the interface irregularities on G_I becomes negligible. In this situation, the diffusing species can have free access to the entire perimeter L_p of the active interface. As a consequence, the reaction rate in the cell should be solely controlled by the parameter K_s. In terms of Λ (the relevant length scale of the system), the conductance of the reactive interface in such *kinetic* regime can be computed as

$$G_K = bK_s L_p = bD\frac{L_p}{\Lambda}. \tag{3}$$

Since this conductance sets an upper limit for the behavior of the reacting cell when there is no diffusion limitation, we can then define at this point the following normalized effectiveness index for the irregular interface:

$$\eta_s(\Lambda) = \frac{G_I}{G_K}. \tag{4}$$

In the next section, we describe how to predict the effectiveness index η_s for arbitrarily irregular catalyst interfaces. This prediction is then checked numerically in Section 2.2.

2.1. The land surveyor approximation

As described in the previous section, to understand the catalytic behavior of irregular interfaces, one has to solve the Laplace equation with boundary conditions like Eq. (1). This is an unsolved mathematical problem. In contrast, the case of Dirichlet boundary condition ($C = 0$) has been thoroughly studied, specially for the case of two-dimensional systems. More specifically, an important theorem proposed by Makarov (Makarov, 1985; Jones & Wolff, 1988) has been used to describe the properties of the current distribution on irregular electrodes, as for example, electrodes which display a fractal geometry at the contact interface. This theorem states that *the information dimension of the harmonic measure on a singly* *connected electrode in $d=2$ is exactly equal to* 1. In the particular case of electrodes, the harmonic measure is the normalized current density, while its counterpart for a diffusion–reaction cell should be the normalized mass flux. In terms of catalytic activity, this special property of the Laplacian field can be illustrated in the following manner: whatever be the shape of the catalyst interface, the total size of the region where most of the reaction takes place, L_{act}, is of the order of the overall size (or diameter) L of the cell under a dilation transformation.

When applied to a transport system like the diffusion–reaction cell shown in Fig. 1a, Makarov's theorem has then a simple, but general consequence: the screening effect due to geometrical irregularities of the catalyst interface can be characterized in terms of the ratio (Sapoval, 1994)

$$S \equiv L_p/L. \tag{5}$$

Since the active length of the interface $L_{\text{act}} \approx L$, then $L_{\text{act}} = L_p/S$ and the factor S can be considered as the "screening factor" of the Dirichlet–Laplacian field. However, this result cannot be applied as such to a diffusion–reaction cell with finite K_s because the boundary condition at the reacting interface is not $C=0$, but $\partial C/\partial n = C/\Lambda$ instead.

To account for the more realistic boundary condition $\partial C/\partial n = C/\Lambda$, we use the LSA. This technique has been originally developed to access the response of an arbitrary irregular electrode from its geometry alone (Sapoval, 1994, 1996). In what follows, we briefly introduce the LSA and show that it can also be used to compute the effectiveness η_s directly from the interface shape at any diffusion–reaction condition, as specified by the physico-chemical parameter Λ. The idea consists of substituting the problem of Laplacian transfer across the *real* interface for *finite* reactivity by a Laplacian field obeying the Dirichlet boundary condition, $C=0$, on a fictitious geometry. This new geometry is obtained through a coarse graining of the real geometry to a physical scale determined by the length Λ. One can then use the screening efficiency of the coarse-grained geometry to find the size of the active zone, hence the activity of the catalyst interface.

More precisely, we consider a region of perimeter δs around the curvilinear coordinate s along the catalyst interface. It displays an elementary reactive conductance $G_{\text{surf}} = [bK_s]\delta s$ which is smaller than the *local access conductance* of order bD. This conductance quantifies the diffusive mass transport at the small square bulk area which is nearby the part of the interface with perimeter length δs. The value of this local access conductance does not depend on the diameter of this area since the conductance of a square of solution with thickness b is equal to $G_{\text{acc}} = bD$ whatever be its size. One can then consider a larger region between curvilinear abscissa s_1 and s_2. Depending on s_1 and s_2, there exist two situations: if the curvilinear distance between s_1 and s_2 is small, the flux of mass is limited by the surface resistance. Such an element works then uniformly. On the contrary, if this distance is large enough, the flux is limited by the bulk resistance to access the surface, and such an object does not work uniformly. But in the latter situation, we are, in a first approximation, back to the case of a pure Laplacian field with the boundary condition $C=0$, since it is the access to the surface that limits the transport of mass.

As shown in Fig. 1b, the coarse graining of the real geometry is locally performed to a scale such that the perimeter $L_{p1} = (s_2 - s_1)$ in a region of size (or diameter) L_{c1} is given by the condition that the local surface reactivity $bK_s(s_2 - s_1)$ along that part of the perimeter is equal to the access conductance $G_{\text{acc}} = bD$. This means that the curvilinear distance $(s_2 - s_1)$ along the catalyst surface is equal to Λ. The chord length $L_c(s)$ is thus defined as the ordinary distance between s_1 and s_2 in real space. From its definition, a coarse-grained region can be considered as working uniformly. At the same time, in the new coarse-grained geometry, we are dealing with a pure Dirichlet–Laplacian field. We then shift from the real geometry to the coarse-grained geometry which is made of successive chords $L_{c1} = L_c(s_0, s_1)$, $L_{c2} = L_c(s_1, s_2), \ldots$ (see Fig. 1b). This operation can be performed whatever the value of Λ, provided that the structure conserves aspect ratios of order one at all scales.

Now, if we observe that the perimeter of the coarse-grained interface is $L_{p,cg} = L_{c1} + L_{c2} + \cdots = N\langle L_c\rangle$, where $\langle L_c\rangle$ is the average chord length, it is possible to express the corresponding screening factor of the coarse-grained geometry as $S_{cg} = L_{p,cg}/L = N\langle L_c\rangle/L$. In this way, the effective conductance can be written as the product of the conductance of the unscreened surface, L_pK_s, by $1/S_{cg}$,

$$G_I = \frac{bL_pK_sL}{N\langle L_c\rangle}. \tag{6}$$

By definition, since each chord corresponds to a perimeter Λ, we can write $L_p = N\Lambda$. After substituting this into Eq. (6), the conductance of the reactive interface can be expressed as (Sapoval et al., 1999)

$$G_I = bD\frac{L}{\langle L_c\rangle}. \tag{7}$$

Eq. (7) indicates that the conductance of a typical wall element can be simply calculated as the local access conductance of the solution bD times the number of chords needed to measure the size (or diameter) L of the interface. This result expresses how the conductance of the diffusion–reaction cell should depend on the *diffusivity* of the reactant species in the bulk phase and the average chord length corresponding to a perimeter of length

$\Lambda \equiv D/K_s$. The geometry enters through the relation between a perimeter of length Λ and its associated chord length.

At this point, it is useful to define from Eq. (7) an *effective reaction rate coefficient* for the interface in terms of $\langle L_c \rangle$ as

$$K_{\text{eff}} = D/\langle L_c \rangle. \tag{8}$$

Finally, from Eqs. (4) and (7), the effectiveness of the system can be expressed as

$$\eta_s = \frac{\Lambda}{S\langle L_c \rangle}. \tag{9}$$

Note that for $\Lambda = L_p$, it follows that $\langle L_c \rangle = L$, and therefore the surface effectiveness reaches its maximum value, $\eta_s = 1$.

The above result (9) is general. It applies to arbitrary wall geometries provided that the wall itself does not present deep pores (Sapoval et al., 1999). In the particular case where the wall irregularity can be described by a fractal geometry, the chord length $\langle L_c \rangle$ of a self-similar interface with dimension D_f, size L and lower cut-off length scale ℓ can be expressed approximately as (Mandelbrot, 1982)

$$\langle L_c \rangle = \begin{cases} \Lambda & \text{if } \Lambda \ll \ell, \\ \ell(\Lambda/\ell)^{\frac{1}{D_f}} & \text{if } \ell < \Lambda < L_p, \\ \Lambda/S & \text{if } \Lambda \gg L_p. \end{cases} \tag{10}$$

Note that, in the case where $\Lambda \gg L_p$, the effective reaction rate coefficient is given by

$$K_{\text{eff}} = SK_s. \tag{11}$$

This exact relation provides a very simple expression for the effect of the roughness on the effective reaction rate.

2.2. Comparison of the land surveyor approximation with the direct 2D numerical solution

As an appropriate test for the quality of the LSA in comparison with direct numerical simulations, we investigate the chemical reaction activity of a non-deterministic self-similar interface, namely, the random Koch curve (RKC). Like the standard Koch curve (Mandelbrot, 1982), the next generation of an RKC is constructed by replacing the middle third of each elementary segment of size ℓ composing the set in the previous generation, by two segments of equal length ($\ell/3$). While the consecutive angles between each pair of remaining and new segments are the same (e.g., -120° or 120°) for all segments in a given iteration and kept the same from generation to generation in the standard Koch curve, they are randomly chosen with equal probability in the case of the RKC. As shown in Fig. 2, the result from this simple iterative process for a four generation RKC is a more realistic interface with a highly "irregular" geometry that still preserves the fractal dimension of the original Koch curve, $D_f = \log 4/\log 3$.

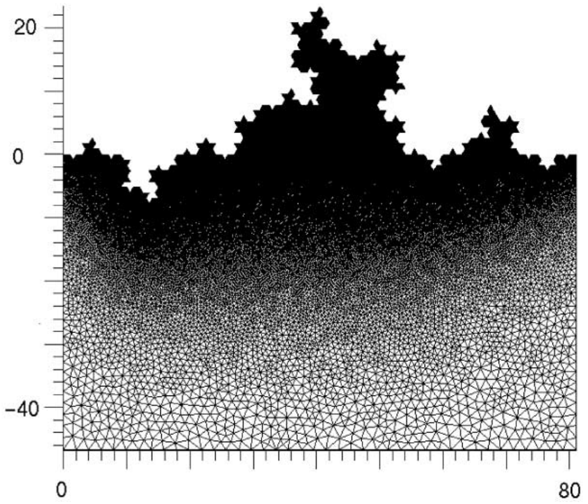

Fig. 2. Typical 4-generation random Koch curve (RKC) used in the simulation of a catalytic interface. Also shown is the unstructured mesh adopted in the finite elements computations.

The numerical solution of the Laplacian problem $\nabla^2 C = 0$ for the concentration field C and overall conductance G_{cell} in a diffusion–reaction cell of arbitrary shape is obtained here through discretization by means of the finite elements technique. For this, we use the Finite Element Library MODULEF (Bernadou et al., 1985). Structured grids comprising quadrilateral elements are very difficult to create when complex geometries are involved (e.g., the rough catalyst interface). To solve this problem, we generate unstructured meshes based on triangular grid elements of a Delaunay network (see Fig. 2). A scheme based on this triangular mesh and P_1-Lagrange interpolation is then applied to discretize the standard variational formulation of the problem. Finally, the resulting linear system of algebraic equations is solved using the Cholesky method. In Fig. 3 we show the concentration field calculated numerically for a typical RKC interface at $\Lambda/\ell = 10$. From the solution for the concentration field for a given value of Λ, we compute G_{cell}. Knowing G_B (the overall conductance of the cell subjected to the condition $C = 0$ at the interface), the conductance G_I and the interface effectiveness η_s can be readily calculated from Eqs. (2) and (4), respectively.

The results shown in Fig. 4 indicate how the effectiveness η_s of the interface depicted in Fig. 2, calculated both from direct numerical simulations and the LSA, depends on the characteristic diffusion–reaction parameter Λ. We can clearly observe the existence of three different regimes for the effectiveness η_s of the catalyst interface. Note that the land surveyor method gives naturally the crossover regimes. Therefore, using the notion of chord

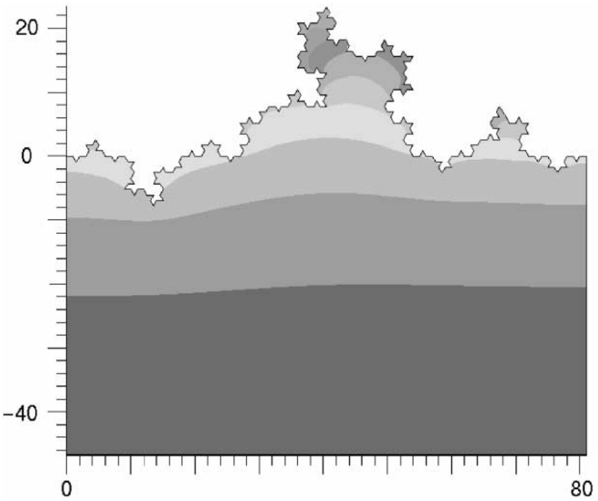

Fig. 3. Steady-state concentration field close to a catalytic interface. The numerical results from finite elements computations have been obtained at diffusion–reaction conditions corresponding to $\Lambda/\ell = 10$. The changes in grey scale correspond to a factor 2 in concentration.

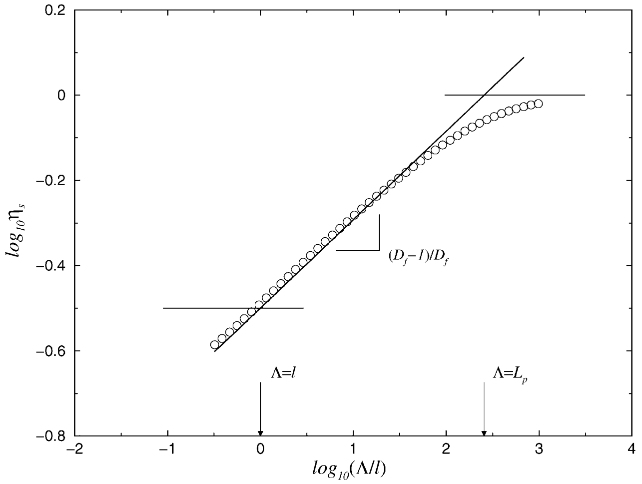

Fig. 4. Logarithmic plot of the effectiveness η_s versus Λ/ℓ for an RKC catalytic interface. The circles correspond to the effectiveness η_s obtained by direct numerical simulation and the solid lines correspond to the LSA predictions given by Eq. (14). The arrows point to the crossovers $\Lambda = \ell$ and $\Lambda = L_p$.

length L_c previously developed to explain geometrically the LSA, it is possible to predict the threefold behavior of η_s. For small values of Λ ($\Lambda \ll \ell$), the chord $\langle L_c \rangle$ should be equal to Λ. From Eq. (9), we obtain directly the result that the interface effectiveness should be given by

$$\eta_s = \frac{1}{S}. \tag{12}$$

We call this lower limit regime of constant effectiveness *the Makarov regime*, because the distribution of the concentration field is very close to that of a Laplacian problem with Dirichlet boundary conditions ($C = 0$). As already pointed out, for a finite value of the diffusion coefficient D, this situation corresponds to the response of a highly reactive interface ($K_s \to \infty$). Of course, the prediction (12) is only approximate because it uses a simplistic interpretation of the Makarov theorem, namely, that the length of the active zone is equal to L, whereas the correct statement should be that the length of the active zone is of the order of L. This is due to the fact that the distribution of mass fluxes over the reactive interface is not uniform (Sapoval et al., 1999).

As shown in Fig. 4, while the LSA predicts accurate values for both the crossover length ℓ and the effectiveness η_s at the Makarov regime, the results from direct numerical simulations underestimate the reactive behavior of the interface. The numerical study of the Makarov regime for the interface shown in Fig. 2 would require at least 100 sites covering the smaller feature ℓ of the irregular geometry to be able to reach the continuous limit. The total linear size of the mesh would then be of order $100(L/\ell) \times 100(L/\ell)$, a very large number, making the computations not feasible. In a previous study (Sapoval et al., 1999), extensive numerical simulations have been performed to closely verify the theory and investigate the transport process in the Makarov regime. As a matter of fact, the Makarov regime is only interesting from a theoretical point of view because real catalyst systems should not operate under significant mass transport limitations. For all these practical and theoretical reasons, we decide to use the finite element technique here with a mesh which is certainly too coarse to study the Makarov regime accurately, but sufficiently refined to investigate the other relevant diffusion–reaction regimes.

At values of Λ larger than the smaller cut-off length ℓ, the general agreement between the effectiveness numerically calculated and predicted by the LSA is fairly good. In the intermediate range $\ell < \Lambda < L_p$, the irregular aspect of the interface has a strong influence on its diffusion–reaction properties. Due to the fractal nature of the particular geometry investigated here, we should then expect the effectiveness η_s to follow a typical power law behavior, as indeed is the case for both numerical calculations and LSA predictions. Again, we follow the same procedure based on the chord length concept to predict, substituting Eq. (10) into Eq. (9), the effectiveness behavior of the interface at the "fractal" regime (i.e., $\ell < \Lambda < L_p$),

$$\eta_s = \frac{1}{S}\left(\frac{\Lambda}{\ell}\right)^{(D_f-1)/D_f}. \tag{13}$$

Therefore, the exponent $(D_f - 1)/D_f$ (≈ 0.207 for the RKC) quantifies an "anomalous" diffusion–reaction behavior for the effectiveness of the catalyst interface.

Now, two relevant points should be addressed from this result. First, if we assume that the intrinsic reactivity

K_s is a thermally activated quantity with energy E_{act}, the effectiveness of the wall element η_s should exhibit, on its turn, an effective activation energy of $(D_f - 1)E_{\text{act}}/D_f$, a value which can be very different from the intrinsic one, E_{act}. Second, the fractal geometry is used here as a paradigm because it permits us to predict analytically the behavior of the effectiveness η_s. For nonfractal irregular geometries, the LSA still applies and Eq. (9) can be used quite generally.

In the regime of maximum interface activity, $\Lambda \gg L_p$, the diffusion mechanism of mass transport in the bulk of the cell offers negligible resistance to the chemical reaction at the interface. As already discussed, this is the point where the reactant species can have free access to all interface sites. In other words, the system reaches a state in which $G_I = G_K$ and therefore the catalyst effectiveness of the system is maximum, $\eta_s = 1$.

Finally, we summarize this section providing the following picture for the diffusion–reaction behavior of an irregular wall element with fractal geometry in terms of its catalyst effectiveness η_s:

$$\eta_s = \begin{cases} 1/S & \text{if } \Lambda \ll \ell, \\ \frac{1}{S}(\frac{\Lambda}{\ell})^{(D_f-1)/D_f} & \text{if } \ell < \Lambda < L_p, \\ 1 & \text{if } \Lambda \gg L_p. \end{cases} \tag{14}$$

2.3. Extension to three dimensions

The same line of reasoning can be used for fractal with $2 \leqslant D_f \leqslant 3$. The screening factor S can be defined as the ratio between the total developed surface A_T and the square of the global size of the element L_A:

$$S = \frac{A_T}{L_A^2}. \tag{15}$$

For a fractal surface of smaller cut-off ℓ, the total surface A_T can be written as

$$A_T = \ell^2 \left(\frac{L_A}{\ell}\right)^{D_f}. \tag{16}$$

The chord length $\langle L_c \rangle$ is now defined as the diameter of the area whose planar cross section would have a perimeter of order Λ (Sapoval, 1996). In this case, the effectiveness takes the following values:

$$\eta_s = \begin{cases} 1/S & \text{if } \Lambda \ll \ell, \\ \frac{1}{S}(\frac{\Lambda}{\ell})^{\frac{D_f-2}{D_f-1}} & \text{if } \ell < \Lambda < \frac{A_T}{L_A}, \\ 1 & \text{if } \Lambda \gg \frac{A_T}{L_A}. \end{cases} \tag{17}$$

In the following, we will study the case of a slit-shaped pore for which an analytical theory can be given and compared to 2D numerical simulations.

3. The catalytic effectiveness of rough pores

In order to demonstrate that the potential applicability of the LSA can go beyond the prediction of the catalyst effectiveness of irregular interfaces, we show here that the methodology used in the previous section can be consistently extended to the study of the catalyst effectiveness of deep rough pores. The basic idea is to consider the linear diffusion transport of reactant A in a single slit-shaped pore of nominal length L_T (x-direction). The two reactive walls of this pore are rough surfaces of thickness b separated by a distance w (y-direction). By definition, they are generated through the translation along b (z-direction) of two lines made by the connection of several wall elements. In particular, we could consider that these elements are similar and have a fractal geometry like the RKC exhibited in Fig. 2. From a source at the pore entrance, molecules of species A diffuse into the pore to react at the walls according to a first-order kinetics.

At first we assume that the pore length is sufficiently large compared to its width ($L_T \gg w$) and the size of the interface unit ($L_T \gg L$). In an one-dimensional approximation, the following differential equation expresses the mass conservation of the reactant in the pore at steady state:

$$\frac{d^2C}{dx^2} - \frac{2K_{\text{eff}}}{Dw}C = 0. \tag{18}$$

Substituting Eq. (8) into Eq. (18), we obtain

$$\frac{d^2C}{dx^2} - \frac{2}{\langle L_c \rangle w}C = 0. \tag{19}$$

Finally, we assume that the source of mass at the pore inlet has a constant concentration C_S and that the pore outlet is nonreactive and closed to the diffusive transport of species A. As a consequence, the boundary conditions for this system can be written as

$$C(0) = C_S \quad \text{and} \quad \left.\frac{dC}{dx}\right|_{x=L_T} = 0. \tag{20}$$

The standard way to quantify the effect of diffusion in heterogeneous catalysis is to define an *effectiveness factor* as (Bird et al., 1960)

$$\eta \equiv \frac{\text{actual mass flow}}{\text{mass flow without diffusion limitations}} = \frac{\Phi}{\Phi_{\max}}. \tag{21}$$

In the case of a first-order reaction and in the absence of diffusion limitations, the mass flow penetrating the system is

$$\Phi_{\max} = \frac{2Db}{\Lambda} L_T S C_S. \tag{22}$$

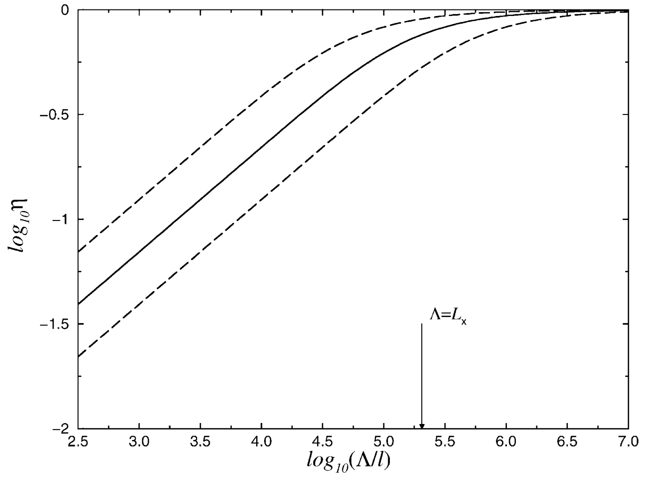

Fig. 5. Logarithmic plot of the effectiveness factor η versus Λ/ℓ. The solid thick line corresponds to the predictions of the LSA for the catalytic behavior of an one-dimensional rough pore whose reactive walls are composed of several 4-generation RKCs. The relevant dimensions of the pore are $w = L$ and $L_T = 20w$. The arrow points to the crossover $\Lambda = L_\times$. For comparison, we also show the curves corresponding to the behavior of smooth pores (dashed lines) with lengths L_T (top) and $L_T S$ (bottom).

From the solution of Eq. (19) subjected to (20), one can compute the mass flow at the pore inlet,

$$\Phi = -\, wbD \left.\frac{\partial C}{\partial x}\right|_{x=0}, \tag{23}$$

to express the effectiveness factor of a rough pore as

$$\eta = \frac{w\Lambda}{2SL_T}(\langle L_c\rangle w/2)^{-1/2}\tanh[(\langle L_c\rangle w/2)^{-1/2}L_T]. \tag{24}$$

This expression applies to any geometry. In this way, the notion of chord length can be directly applied to this problem. The irregularity enters through the dependence of $\langle L_c\rangle$ on $\Lambda \equiv D/K_s$.

In the particular case of a fractal, we can use Eq. (10) as an approximate description for the general variation of the length $\langle L_c\rangle$ in terms of its *intrinsic* counterpart Λ. However, for the one-dimensional description to remain valid, the inequalities $L > w$ and $(\langle L_c\rangle w)^{1/2} > L$ must hold. As a consequence, our analysis becomes restricted to diffusion–reaction conditions in the range $\Lambda > L_p$. Fig. 5 shows the predictions from Eqs. (10) and (24) for the behavior of the catalyst effectiveness η of a rough pore generated from a series of connected fractal interfaces of dimension $D_f = \log 4/\log 3$ (in particular, the behavior shown in Fig. 5 corresponds to the case of a standard Koch curve or a RKC). For comparison, the classical effectiveness behaviors of smooth pores with lengths L_T and $L_T S$ are also displayed in Fig. 5.

In the limit of negligible resistance to pore diffusion, the catalytic effectiveness of the system approaches asymptotically its maximum, $\eta = 1$. From Eq. (21) and the prediction of $\langle L_c\rangle$ from Eq. (10) for $\Lambda > L_p$, this saturation regime should hold for

$$\Lambda > L_\times \equiv 2L_T^2 S/w. \tag{25}$$

The length scale $L_\times$ determines the crossover between strong to weak resistance to pore diffusion in the rough pore. It is important to note at this point that, differently from the classical behavior of a smooth pore, $L_\times$ includes a correction S due to the irregularities (i.e., roughness) of the pore walls, *whether these irregularities are fractal or not*.

If we now substitute Eq. (10) into Eq. (24) for $\Lambda > L_p$, the following expression is obtained for the variability of η in the range $L_p < \Lambda < L_\times$:

$$\eta = \left(\frac{w\Lambda}{2S}\right)^{1/2}\frac{1}{L_T}. \tag{26}$$

This equation simply indicates that, although the activity of the wall is locally maximized at these diffusion–reaction conditions, the deeper part of the pore cannot be reached by reactant molecules either due to strong diffusion resistance at the pore level or high reaction activity at the pore surface. As a consequence, the classical behavior for diffusion and reaction should be observed, $\eta \propto \Lambda^{1/2}$. From a practical point of view, however, this classical diffusion behavior should be distinguished from the one exhibited by a smooth pore (see Fig. 5). In reality, these two regimes can operate in a quite different range of Λ values, depending on the factor S.

We turn now to the investigation of the effectiveness of rough pores where the assumption $L_T \gg w$, originally taken to consider the simplified one-dimensional case, is now relaxed to account for two-dimensional effects. The following differential equation should then provide an approximate description for the diffusion–reaction phenomena in a slit-shaped rough pore:

$$\frac{\partial^2 C}{\partial x^2} + \frac{\partial^2 C}{\partial y^2} = 0, \tag{27}$$

with boundary conditions given by

$$C(0,y) = C_S, \quad \frac{\partial C}{\partial x}(L_T, y) = 0, \quad \frac{\partial C}{\partial y}(x,0) = 0$$

and

$$\frac{\partial C}{\partial y}(x, w/2) + \frac{K_{\mathrm{eff}}}{D}C(x, w/2) = 0. \tag{28}$$

The third boundary condition shown above corresponds to the assumption that the pore is symmetric with respect to $y = 0$. From the solution of Eq. (27) subjected to Eq. (28) (Carslaw & Jaeger, 1959), we can calculate

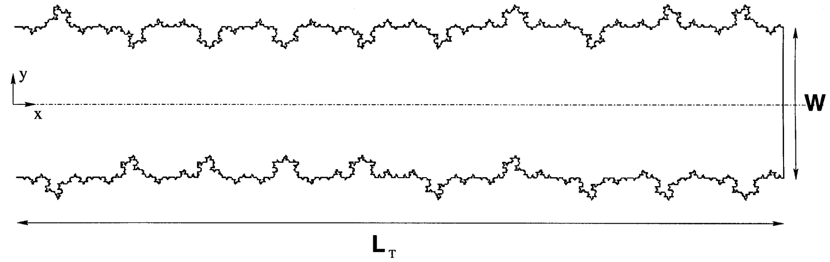

Fig. 6. Schematic representation of the two-dimensional rough pore used in the simulations. Each of the two reactive walls are composed of 10 RKCs of three generations.

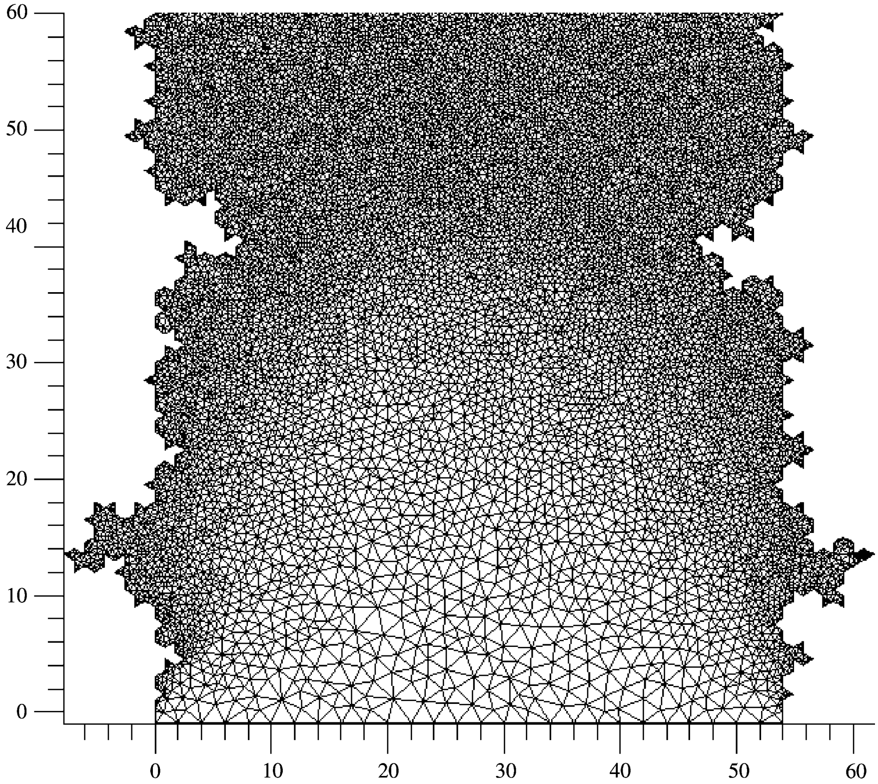

Fig. 7. Subset of the two-dimensional rough pore showing the unstructured numerical mesh used in the finite elements computations of the diffusion–reaction process.

the mass flow penetrating the system,

$$\Phi = 2b\int_0^{\frac{w}{2}}\left[-D\frac{\partial C}{\partial x}(0,y)\right]\,\mathrm{d}y \tag{29}$$

to obtain, by means of Eq. (8), Eq. (22) and the previous definition (21), the following expression for the catalytic effectiveness of a two-dimensional rough pore:

$$\eta = \frac{2\Lambda}{\langle L_c\rangle L_T S}\sum_{n=1}^{\infty}\frac{\tan(\alpha_n w/2)\tanh(\alpha_n L_T)}{[(\alpha_n^2+\langle L_c\rangle^{-2})w/2+\langle L_c\rangle^{-1}]}, \tag{30}$$

where α_n is the nth root of the eigenvalue equation,

$$\alpha_n\tan(\alpha_n w/2) = \langle L_c\rangle^{-1} \quad \text{for } n = 1,2,3,\ldots\,. \tag{31}$$

In order to check the validity of Eq. (30) in combination with the prediction given by Eq. (10) for the active length $\langle L_c\rangle$, we used a numerical scheme entirely similar to the one described in Section 2 for active interfaces, but now applied to generate the solution of the two-dimensional Laplacian transport in a rough pore geometry whose active walls are composed of several elementary RKC interfaces. Due to computational limitations, however, here we restricted our simulations to reactive pore walls made by RKC curves of only three generations (see Fig. 6). As shown in Fig. 7, a very refined mesh is used to produce accurate results in terms of effectiveness factors at various diffusion–reaction conditions. In Figs. 8a and b, we show the

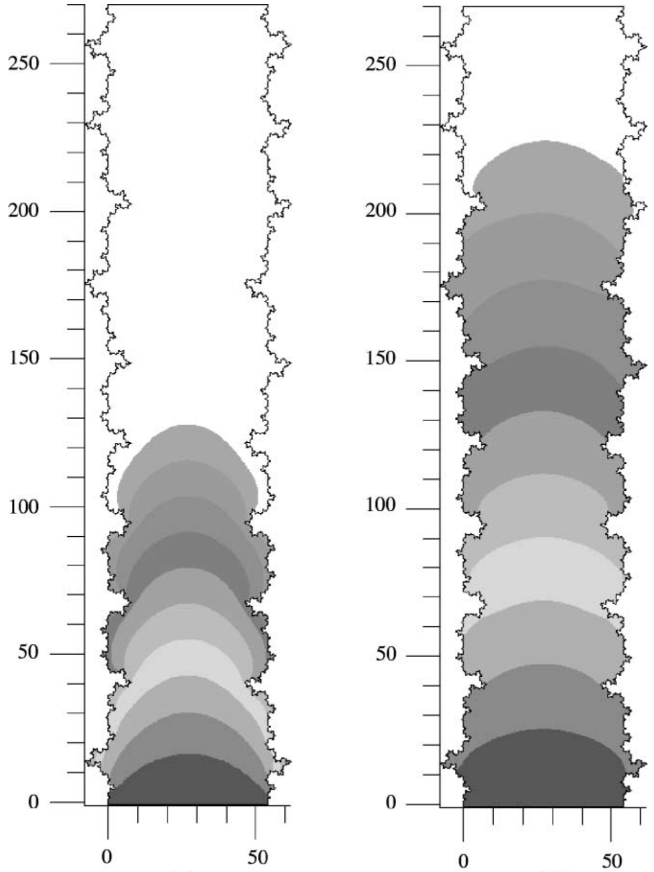

(a) (b)

Fig. 8. (a) Steady-state concentration field of reactant penetrating a catalytic rough pore for $\Lambda/\ell = 10$. (b) Same as in (a), but for $\Lambda/\ell = 100$. These contour plots have been computed from direct numerical simulation using the finite elements technique. The change in the grey scale corresponds to a factor of 2 in concentration.

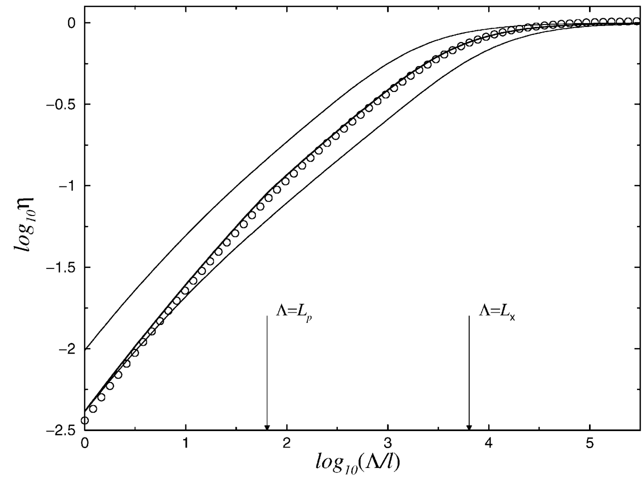

Fig. 9. Dependence of the effectiveness factor η on Λ/ℓ for a two-dimensional catalytic rough pore. The dimensions of the pore are $w = 2L$ and $L_T = 10L$ and $L_p/L = S = 64/27$. The circles correspond to η values calculated from direct numerical simulation of the rough pore shown in Fig. 8 under different diffusion–reaction conditions. The thick solid line is the analytical prediction from Eqs. (10) and (30) for the catalytic effectiveness. The arrows point to the crossovers $\Lambda = L_p$ and $\Lambda = L_\times$. For comparison, we also show the two curves corresponding to the behavior of two-dimensional smooth pores (thin lines) with lengths L_T (top) and L_TS (bottom).

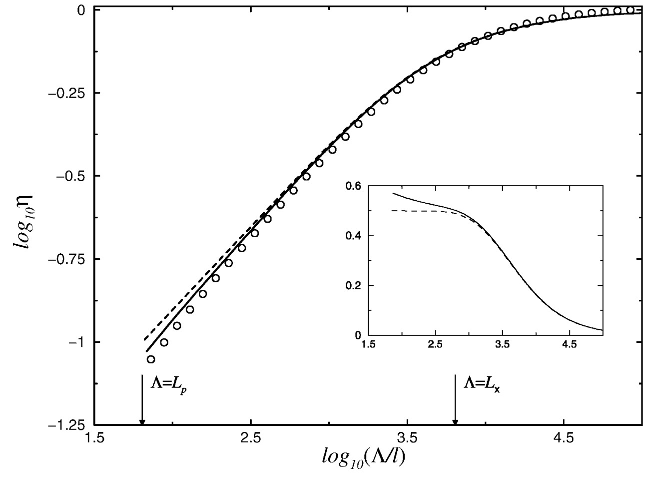

Fig. 10. Comparison between the one- and two-dimensional LSA predictions for the pore considered in Fig. 9. The circles correspond to η values calculated from direct numerical simulation of the rough pore and the thick solid line is the prediction from Eqs. (10) and (30). The dashed line is the prediction from the one-dimensional approximation (24) and the arrows point to the crossovers $\Lambda = L_p$ and $\Lambda = L_\times$. The inset shows two curves corresponding to the derivatives in the main graph of the predictions from the one-dimensional approximation (dashed line) and the two-dimensional model (solid line).

concentration fields numerically calculated for $\Lambda/\ell = 10$ and 100, respectively.

The results displayed in Fig. 9 show that the LSA predictions are in excellent agreement with the numerical simulations of the diffusion–reaction phenomenon in a two-dimensional rough pore, over the whole range of relevant η variability, namely, for $\Lambda/\ell > 1$. Finally, it is interesting to compare the results obtained for a rough pore with the classical behavior of reactive, but flat pores. Also shown in Fig. 9 are the logarithmic curves of η versus Λ for two-dimensional smooth pores with lengths L_T and L_TS. The large discrepancy which can be observed among the behaviors of rough and flat pores indicates the important role played by the geometry of the catalytic interfaces.

For the sake of comparison, we show in Fig. 10 that, if the catalytic pore is sufficiently deep, the one-dimensional approximation given by Eq. (30) can still provide a satisfactory prediction for the effectiveness factor in the range $\Lambda > L_p$. One should note, however, that deviations from the behavior $\eta \propto \Lambda^{1/2}$ due to two-dimensional effects become more evident as Λ decreases and approaches L_p. As shown in the inset of Fig. 10, this difference can be better visualized if we follow the behavior of the derivatives taken from the curves in the main graph.

4. Conclusions

In addition to several studies revealing the strong influence of the pore space morphology on the global efficiency of a diffusion–reaction system (Sharrat & Mann, 1987; Hollewand & Gladden, 1992; Mann, 1993; Zhang & Seaton, 1994), the present work provides clear evidence that this effect is not only relevant, but should, as a matter of fact, govern the catalytic activity of irregular interfaces under diffusion limitations. Indeed, our results indicate that the knowledge of the interface geometry is sufficient to provide accurate predictions for the catalytic activity over a wide range of diffusion–reaction conditions. Extensive numerical simulations have been carried out to demonstrate that analytical predictions using the land surveyor approximation (LSA) are good enough to estimate the catalytic effectiveness of one- and two-dimensional rough pores with a high degree of accuracy, in the presence or absence of screening effects. In spite of the complex morphological features a pore might possess, it appears that the geometrical information necessary to characterize the roughness of its reactive walls is sufficient to predict its catalytic effectiveness. What really counts here is the screening factor S, the ratio between the real and the apparent surface area of the pore, whatever the underlying geometrical details. Indeed, it has been shown recently that random and deterministic fractal interfaces with the same fractal dimension display the same transport properties (Filoche & Sapoval, 2000a). We expect this result to be valid for real porous catalysts.

Another result of potential interest from this study is the remarkable difference one can detect by comparing the effectiveness behavior of a pore with smooth active walls and a given nominal length (in fact, an *apparent* effectiveness factor) and a pore with the same nominal length, but with rough catalytic surfaces. We argue that this, among other factors like the complex structure of the pore space (McGreavy et al., 1992), could contribute to the significant discrepancies previously found between experimental measurements and the standard theoretical approach using effective diffusion coefficients (McGreavy & Siddiqui, 1980). It is important to note, however, that the molecular diffusion approximation employed here can only be locally valid inside of a bulk void space between protrusions if the mean free path of the diffusing reactant is sufficiently smaller than the width of this interstitial region. The molecular mean free path constitutes a lower cut-off for the validity of our description. If the surface would present smaller geometrical features, it would result in an equivalent intrinsic reactivity determined by the Knudsen regime as studied by Coppens and Froment (1995a, b) and Santra and Sapoval (1999).

We believe that the LSA approximation in combination with the modeling techniques presented here can be a useful tool to provide some interesting guidelines for the design problem of a suitable catalyst porous structure for a given reactive system. Moreover, the approach introduced in this study is certainly flexible enough to represent more specific geometrical characteristics of irregular pore spaces as well as other types of reaction mechanisms (e.g., higher-order kinetics) limited by diffusion transport. In particular, recent studies have shown that the LSA can be also applied to surfaces with nonuniform activities (Filoche & Sapoval, 1997) and nonlinear reaction rate mechanisms (Filoche & Sapoval, 2000b).

A remarkable result here is that the screening factor S, which has a simple geometrical meaning and can be measured by electron microscopy or small angle X-ray scattering, plays a fundamental role in determining the catalytic efficiency of deep rough pores. One should note that, for an arbitrary random interface, the factor S should be measured as the perimeter to size ratio in a region with a size of the order or larger than the correlation length of the geometry. Such a region constitutes a typical wall element. Also, for a real three-dimensional pore, the perimeter to be considered is the total length of the cut of the surface by a plane (Sapoval, 1996).

Finally, one should recall that anomalous behaviors (anomalous diffusion (Havlin & Ben-Avraham, 1987; Stauffer & Aharony, 1992; Andrade et al., 1997) or anomalous kinetics (Kopelman, 1989; Ziff et al., 1986)) represent an additional complication factor in the interpretation of experimental data. Our results indicate that, for the particular case of linear kinetics in rough pores, the effect of an irregular geometry is to modify the effective reactivity and not the diffusion transport coefficient.

Notation

b	thickness of the reacting cell, m
C	concentration of reactant, mol/m^3
D	molecular diffusion coefficient, m^2/s
D_f	fractal dimension
K_s	surface reaction rate coefficient, m/s
K_{eff}	effective reaction rate coefficient, m/s
L	length of the catalyst interface, m
L_{act}	active length of the interface, m
L_c	chord length, m
L_p	perimeter of the catalyst interface, m
L_T	pore length, m
S	screening factor
G	surface "conductance", m^3/s
w	pore width, m

Greek letters

Λ	diffusion–reaction length scale, m
η	pore effectiveness
η_s	surface effectiveness
Φ	mass flow, mol/s

Acknowledgements

This work has been partially supported by CNPq.

References

Adler, P. M. (1992). *Porous media: Geometry and transport*. Stoneham MA: Butterworth-Heinemann.

Andrade Jr., J. S., Street, D. A., Shibusa, Y., Havlin, S., & Stanley, H. E. (1997). Diffusion and reaction in percolating pore networks. *Physical Review E*, *55*, 772–777.

Aris, R. (1975). *The mathematical theory of diffusion and reaction in permeable catalysts*. Oxford: Clarendon Press.

Avnir, D. (Ed.). (1989). *The fractal approach to heterogeneous chemistry*: *Surfaces*, *colloids*, *polymers*. Chichester: Wiley.

Bernadou, M., George, P. L., Hassim, A., Joly, P., Laug, P., Perronnet, A., Saltel, E., Steer, D., Vanderborck, G., & Vidrascu, M. (1985). *Modulef: une bibliothèque modulaire d'éléments finis*. France: INRIA.

Bird, R. B., Stewart, W. E., & Lightfoot, E. N. (1960). *Transport phenomena*. New York: Wiley.

Carslaw, H. S., & Jaeger, J. C. (1959). *Conduction of heat in solids*. Oxford: Clarendon Press.

Coppens, M.-O., & Froment, G. F. (1994). Diffusion and reaction in fractal catalyst pore—III. Application to the simulation of vynil-acetate production from ethylene. *Chemical Engineering Science*, *49*, 4897–4907.

Coppens, M.-O., & Froment, G. F. (1995a). Diffusion and reaction in fractal catalyst pore—I. Geometrical aspects. *Chemical Engineering Science*, *50*, 1013–1026.

Coppens, M.-O., & Froment, G. F. (1995b). Diffusion and reaction in fractal catalyst pore—II. Diffusion and first-order reaction. *Chemical Engineering Science*, *50*, 1027–1039.

Coppens, M.-O., & Froment, G. F. (1997). The effectiveness of mass fractal catalysts. *Fractals*, *5*, 493–505.

Coppens, M.-O. (1999). The effect of fractal surface roughness on diffusion and reaction in porous catalysts—from fundamentals to practical applications. *Catalysis Today*, *53*, 225–243.

Elias-Kohav, T., Sheintuch, M., & Avnir, D. (1991). Steady state diffusion and reaction in catalytic porous media. *Chemical Engineering Science*, *46*, 2787–2798.

Filoche, M., & Sapoval, B. (1997). A simple method to compute the response of non-homogeneous and irregular interfaces: electrodes and membranes. *Journal de Physique I France*, *7*, 1487–1498.

Filoche, M., & Sapoval, B. (2000a). Transfer across random versus deterministic fractal interfaces. *Physical Review Letters*, *84*, 5776–5779.

Filoche, M., & Sapoval, B. (2000b). Shape-dependency of current through non-linear irregular electrodes. *Electrochimica Acta*, *46*, 213–220.

Froment, G. F., & Bischoff, K. B. (1990). *Chemical reactor analysis and design*. New York: Wiley.

Gavrilov, C., & Sheintuch, M. (1997). Reaction rates in fractals vs. Uniform catalysts with linear and nonlinear kinetics. *A.I.Ch.E. Journal*, *43*, 1691–1699.

Giona, M. (1992). First-order reaction-diffusion kinetics in complex fractal media. *Chemical Engineering Science*, *47*, 1503–1515.

Gutfraind, R., Sheintuch, M., & Avnir, D. (1991). Fractal and multifractal analysis of the sensitivity of catalytic reactions to catalytic structure. *Journal of Chemical Physics*, *95*, 6100–6111.

Gutfraind, R., & Sheintuch, M. (1992). Scaling approach to study diffusion and reaction processes on fractal catalysts. *Chemical Engineering Science*, *47*, 4425–4433.

Havlin, S., & Ben-Avraham, B. (1987). Diffusion in disordered media. *Advances in Physics*, *36*, 695–798.

Hollewand, M. P., & Gladden, L. F. (1992). Modelling of diffusion and reaction in porous catalysts using a random three-dimensional network model. *Chemical Engineering Science*, *47*, 1761–1770.

Jones, P., & Wolff, T. (1988). Hausdorff dimension of harmonic measures in the plane. *Acta Mathematica*, *161*, 131–144.

Keil, F. (1996). Modelling of phenomena within catalyst particles. *Chemical Engineering Science*, *51*, 1543–1567.

Kopelman, R. (1989). In D. Avnir (Ed.), *The fractal approach to heterogeneous chemistry*. New York: Wiley.

Makarov, N. G. (1985). On the distortion of boundary sets under conformal mapping. *Proceedings of the London Mathematical Society*, *51*, 369–384.

Mandelbrot, B. B. (1982). *The fractal geometry of nature*. San Francisco: Freeman.

Mann, R. (1993). Developments in chemical reaction engineering: Issues relating to particle pore structures and porous materials. *Transactions of the Institution of Chemical Engineers*, *41*, 711–718.

McGreavy, C., & Siddiqui, M. A. (1980). Consistent measurement of diffusion coefficients for effectiveness factors. *Chemical Engineering Science*, *35*, 3–9.

McGreavy, C., Andrade Jr., J. S., & Rajagopal, K. (1992). Consistent evaluation of effective diffusion and reaction in pore networks. *Chemical Engineering Science*, *47*, 2751–2756.

Meakin, P. (1986). Simulation of the effects of fractal geometry on the selectivity of heterogeneous catalysts. *Chemical Physics Letters*, *123*, 428–432.

Mougin, P., Pons, M., & Villermaux, J. (1996). Reaction and Diffusion at an artificial fractal interface: evidence for a new diffusional regime. *Chemical Engineering Science*, *51*, 2293–2302.

Pfeifer, P., & Sapoval, B. (1995). Optimization of diffusive transport to irregular surfaces with low sticking probability. *Materials Research Society Symposium Proceedings*, *366*, 271–276.

Sahimi, M. (1995). *Flow and transport in porous media and fractured rock*. Boston: VCH.

Santra, S. B., & Sapoval, B. (1999). Interaction of ballistic particles with irregular walls, Knudsen diffusion, and catalytic efficiency. *Physical Review E*, *57*, 6888–6896.

Seri-Levy, A., & Avnir, D. (1991). Fractal analysis of surface geometry effects on catalytic reactions. *Surface Science*, *248*, 258–270.

Sapoval, B. (1994). General formulation of Laplacian transfer across irregular surfaces. *Physical Review Letters*, *73*, 3314–3316.

Sapoval, B. (1996). Transport across irregular interfaces: Fractal electrodes, membranes and catalysts. In A. Bunde, & S. Havlin (Eds.), *Fractals and disordered systems* (pp. 232–261). Berlin: Springer.

Sapoval, B., Filoche, M., Karamanos, K., & Brizzi, R. (1999). Can one hear the shape of an electrode? I. Numerical study of the active zone in Laplacian transfer. *European Physics Journal B*, *9*, 739–753.

Sharrat, P. N., & Mann, R. (1987). Some observations on variation of tortuosity with Thiele modulus and pore size distribution. *Chemical Engineering Science*, *42*, 1565–1576.

Stauffer, D., & Aharony, A. (1992). *Introduction to Percolation Theory*. London: Taylor & Francis.

Thomas, J. M., & Thomas, W. J. (1997). *Principles and practice of heterogeneous chemistry*. Weinheim: VCH.

Villermaux, J., Schweich, D., & Authelin, J.-R. (1987). Transfert et réaction à une interface fractale représentée par le ≪Peigne du Diable≫. *C. R. Acad. Sci. Paris Série II*, *304*, 399–404.

Ziff, R. M., Gulari, E., & Barshad, Y. (1986). Kinetic phase transition in an irreversible surface-reaction model. *Physical Review Letters*, *56*, 2553–2556.

Zhang, L., & Seaton, N. A. (1994). The application of continuum equations to diffusion and reaction in pore networks. *Chemical Engineering Science*, *49*, 41–50.